土木学会論文集 A2(応用力学), Vol. 72, No. 2 (応用力学論文集 Vol. 19), I_495-I_504, 2016.

Simulation of the erosion and seepage failure around sheet pile using two-phase WC-SPH method

Ahmed M. ABDELRAZEK[1, 4], Ichiro KIMURA[2], and Yasuyuki SHIMIZU[3]

[1]Member of JSCE, Dr. of Eng., Researcher, Hydraulic Research Laboratory, Hokkaido University
(Sapporo, 060-8628, Kita-Ku, Kita-13, Nishi-8, Japan)
E-mail:ahmedmrazek@yahoo.com
[2]Member of JSCE, Dr. of Eng., Associate Professor, Hydraulic Research Laboratory, Hokkaido University
(Sapporo, 060-8628, Kita-Ku, Kita-13, Nishi-8, Japan)
E-mail: i-kimu2@eng.hokudai.ac.jp
[3]Member of JSCE, Dr. of Eng., Professor, Hydraulic Research Laboratory, Hokkaido University
(Sapporo, 060-8628, Kita-Ku, Kita-13, Nishi-8, Japan)
E-mail: yasu@eng.hokudai.ac.jp
[4]Irrigation Eng. & Hydraulic Department, Faculty of Engineering, Alexandria University, Alexandria, Egypt
(Alexandria 11432, Lotfy El-Sied st. off Gamal Abd El-Naser - Egypt)

In this study, a Lagrangian formulation of the Navier–Stokes equations, based on the weakly compressible smoothed particle hydrodynamics (WC-SPH) method, was applied to simulate the seepage failure around sheet-pile. In this simulation, the advantages of SPH will be exploited to simulate the soil–water interaction. Water is considered as a viscous fluid with weak compressibility and soil is assumed to be an elastic–plastic material. The elastic–perfectly plastic model based on Mohr–Coulomb's failure criterion is implemented in SPH formulations to model the soil movement. Interaction between soil and water is taken into account by means of seepage force and pore water pressure. Numerical Simulation of the 2-D classical seepage failure problem of horizontal ground with an embedded sheet pile has been done. The numerical results were verified by comparison with model test results, the results have shown that the proposed model could be considered a powerful tool to simulate extremely large deformation and failure of soil.

Key Words: *Hydrodynamics, SPH method, Seepage failure, Soil-water interaction*

1. INTRODUCTION

When water moves through the soil voids with enough velocity, erosion can occur because of the frictional drag exerted on the soil particles. This kind of vertically upwards forces is a source of danger on the downstream side of sheet piling and underneath the toe of hydraulics structures such as dams, regulators, and Barrages.

Seepage around a sheet - pile considers one of the most important factors that affect the stability and the performance of the cofferdams which commonly used in construction excavations.

There are some traditional numerical methods for deformation and failure of geometries in the framework of continuum mechanics, such as finite element method, finite difference method and boundary element method. These methods have been successfully implemented. On the other hand, in the case of large deformation problems, the previous methods produce instabilities due to excessive distortion of a mesh.

Recently a new class of numerical methods has been developed called mesh-free methods. Mesh-free methods do not require Eulerian grids and they deal with a number of particles in a Lagrangian framework. They are considered to be more effective than traditional methods in dealing with problems involving large deformations. The key idea of these methods is to provide an accurate and a stable numerical solution of the partial differential equations using a set of distributed particles in the domain without using any grid.

Many mesh-free methods have been developed in the last decades, such as, the Moving Particle Semi-implicit Method (MPS), the Diffuse Element Method (DEM), the Element-Free Galerkin Method (EFGM), and the Finite Pointset Method (FPM), etc. Among these methods, the Smoothed Particle Hydrodynamics (SPH) method is widely used.

SPH method is a mesh-free particle method and it is considered to be one of the most modern mesh-free particle techniques. It was originally invented for astrophysical applications [1), 2)]; then it has been applied in a huge range of applications such as dynamic response of material strength [3)], free surface fluid flow [4), 5)], incompressible fluid flow [6) 7)], multi-phase flow [8)], turbulence flow [9)], snow avalanching [10), 11)], and gravity granular rapid flow[12), 13), 14)]. In SPH method, each particle in the domain carries all field variable information such as density, pressure, velocity and it moves with the material velocity. The governing equations in the form of partial differential equations are converted to the particle equations of motion, and then they are solved by a suitable numerical scheme.

In this study, the advantages of SPH will be exploited to simulate the soil–water interaction. Water is considered as a viscous fluid with weak compressibility and soil is assumed to be an elastic–plastic material. The elastic–perfectly plastic model based on Mohr–Coulomb's failure criterion is implemented in SPH formulations to model the soil movement [14), 15)].

Modeling of soil and water in the framework of the smoothed particle hydrodynamics method have been presented and verified as one-phase flow models in the authors' former published papers [5), 13)], however, these models only allow simulating one-phase flow.

In this paper, the proposed SPH model is applied to simulate the classical seepage failure problem of horizontal ground with an embedded sheet pile.

Maeda et al., [16), 17)] used the same method to developed three-phase model: solid (soil), liquid (water) and gas (air), and they applied to simulate seepage failure around sheet pile. However, they didn't consider the effect of water pressure on the soil particles, which always exists in natural saturated soil. Also they used the real value of the soil bulk modulus, which lead to a stiff behavior of soil (increase the pressure fluctuations).

In our model, the interaction between soil and water is taken into account by means of seepage force and pore water pressure in order to conduct two-phase model.

The numerical results are then compared with experimental data. The results got from this comparison indicate that the SPH model SPH could be a very effective method for simulation of complex problem in soil mechanics.

2. SPH SIMULATION METHOD

The SPH method is a continuum-scale numerical method. The material properties $f(x)$, at any point x in the simulation domain are calculated according to an interpolation theory over its neighboring particles which are within its influence domain $\boldsymbol{\Omega}$ as shown in **Fig. 1**, through the following formula,

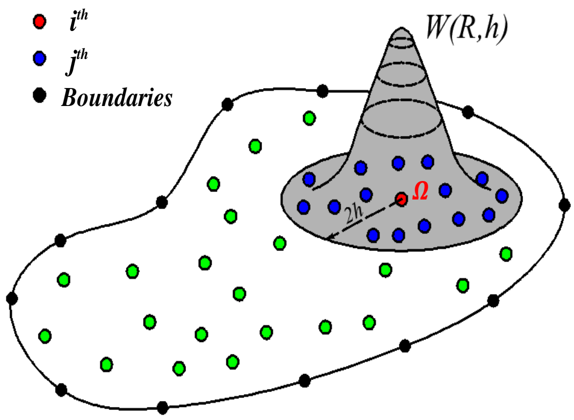

Fig.1 Particle approximation based on kernel function W in influence domain $\boldsymbol{\Omega}$ with radius kh

$$\langle f(x)\rangle = \int_{\Omega} f(x')W(x-x',h)dx' \qquad (1)$$

where h is the smoothing length defining the inflence domain of the kernel estimate and $W(x–x', h)$ is the smoothing function, which must satisfy three conditions [18)]: the first condition is the normalization,

$$\int_{\Omega} W(x-x',h)dx' = 1 \qquad (2)$$

the second one is the Delta function condition,

$$\lim_{h\to 0} W(x-x',h) = \delta(x-x') \qquad (3)$$

and the third condition is the compact condition,

$$W(x-x',h) = 0 \quad \text{when } |x-x'| > kh \qquad (4)$$

where k is constant depending on the type of smoothing function. There are many possible types of smoothing functions, which can satisfy the aforementioned conditions. The most known function, among them, is the cubic spline interpolation function, and quintic wendland kernel. In this study, we used the quintic wendland kernel function which was proposed by Wendland [19)], and it is defined as:

$$W(R,h) = \alpha_d\left(1-\frac{R}{2}\right)^4 (2R+1) \quad 0 \le R \le 2 \quad (5)$$

where $\alpha_d = \frac{7}{4\pi h^2}$ in 2D space, and $R = \frac{(x-x')}{h}$.

In the SPH method, the calculation domain is represented by a finite number of particles, which carry mass and the field variable information such as density, stress, etc. [18].

Accordingly, the continuous integral representation for $f(x)$ is approximated in the following form:

$$\langle f(x)\rangle = \int_{\Omega} f(x')W(x-x',h)dx' \approx \sum_{j=1}^{N} f(x_j)\, W(x-x',h)\frac{m_j}{\rho_j} \quad (6)$$

Equation (7) states that the value of the function at particle *i* is approximated using a weighted average of those values of the function at all other particles in the influence domain of particle *i*. Following the same argument, the particle approximation of the spatial derivative of a function at any particle *i* is,

$$\langle \nabla . f(x_i)\rangle = \sum_{j=1}^{N} \frac{m_j}{\rho_j} f(x_j)\, \nabla_i W_{ij} \quad (8)$$

3. SPH MODEL FOR WATER

For a fluid like water, it is customary to model it as exactly incompressible. However, the approach in SPH is different; the real fluid is approximated by an artificial fluid which is more compressible than the real one, while still possessing a speed of sound which is much larger than the flow speed, and which therefore has very small density fluctuation. The governing equations for fluid flow are the well-known Navier–Stokes equations, which in the Lagrangian description state the conservation of mass and momentum as follows:

$$\frac{D\rho}{Dt} = -\rho \frac{\partial v^{\alpha}}{\partial x^{\alpha}} \quad (9)$$

$$\frac{Dv^{\alpha}}{Dt} = \frac{1}{\rho}\left(\frac{\partial \sigma^{\alpha\beta}}{\partial x^{\alpha}}\right) + f^{\alpha} \quad (10)$$

where α and β denote the Cartesian components *x, y* and *z* with the Einstein convention applied to repeated indices; ρ is the density; v is velocity; $\sigma^{\alpha\beta}$ is stress tensor, f^{α} is the component of acceleration caused by external force, and *D/Dt* is material derivative.

The stress tensor, $\sigma^{\alpha\beta}$, normally consists of two parts: an isotropic pressure *P* and a viscous shear stress, which is proportional to the shear strain rate denoted by ε through the viscosity μ,

$$\sigma^{\alpha\beta} = -P\delta^{\alpha\beta} + \mu\varepsilon^{\alpha\beta} \quad (11)$$

Where:

$$\varepsilon^{\alpha\beta} = \frac{\partial v^{\alpha}}{\partial x^{\beta}} + \frac{\partial v^{\beta}}{\partial x^{\alpha}} - \frac{2}{3}\left(\frac{\partial v^{\gamma}}{\partial x^{\gamma}}\right)\delta^{\alpha\beta} \quad (12)$$

Using the concept of the SPH approximation, the system of partial differential equations (9) and (10) can be converted into the SPH formulations which will be used to solve the motion of fluid particles as follows:

$$\frac{D\rho_i}{Dt} = \sum_{j=1}^{N} m_j (v_i^{\alpha} - v_j^{\alpha}) \frac{\partial W_{ij}}{\partial x_i^{\alpha}} \quad (13)$$

$$\frac{Dv_i^{\alpha}}{Dt} = \sum_{j=1}^{N} m_j \left(\frac{\sigma_i^{\alpha\beta}}{\rho_i^2} + \frac{\sigma_j^{\alpha\beta}}{\rho_j^2}\right)\frac{\partial W_{ij}}{\partial x_i^{\beta}} + f^{\alpha} \quad (14)$$

Similarly, the SPH approximation of shear strain rate $\varepsilon_i^{\alpha\beta}$ for particle *i* is

$$\varepsilon_i^{\alpha\beta} = \sum_{j=1}^{N} \frac{m_j}{\rho_j}(v_i^{\alpha} - v_j^{\alpha})\frac{\partial W_{ij}}{\partial x_i^{\beta}} + \sum_{j=1}^{N} \frac{m_j}{\rho_j}(v_i^{\beta} - v_j^{\beta})\frac{\partial W_{ij}}{\partial x_i^{\alpha}} - \left(\frac{2}{3}\sum_{j=1}^{N} \frac{m_j}{\rho_j}(v_i^{\gamma} - v_j^{\gamma})\frac{\partial W_{ij}}{\partial x_i^{\gamma}}\right)\delta^{\alpha\beta} \quad (15)$$

The final equation needed to solve the above Navier–Stokes equations for water is the ‘‘equation of state’’ which is used to estimate the pressure change of water. Following Monaghan [4] the pressure can be calculated using the equation of Tait:

$$P = B\left[\left(\frac{\rho}{\rho_o}\right)^{\lambda} - 1\right] \quad (16)$$

where λ is a constant (=7) [4], ρ_o is the reference density, *B* is a problem dependent parameter, which sets a limit for the maximum change of the density and will be calculated as

$$B = \frac{100\, V_{type}^2\, \rho_o}{\lambda}\ , V_{type} = \sqrt{2\,\mathrm{g}\,H} \quad (17)$$

where V_{type} is the typical speed of water and *H* is the depth of the water [4].

4. SPH MODEL FOR SOIL

Modeling the behavior of soil using the SPH method is similar to that of water. The SPH form of conservation equations (9) and (10) are still used to estimate the density and motion of soil particles. The key difference between these two models is the calculation of the stress tensor appearing in equation (10) in which the pressure and stress–strain relationship of soil are calculated differently from those of water. The soil is assumed herein to be an elastic–plastic material; the stress tensor of soil is made up of two parts: isotropic pressure P and deviatoric shear stress S,

$$\sigma^{\alpha\beta} = -P\delta^{\alpha\beta} + S^{\alpha\beta} \tag{18}$$

Since soil is assumed to have elastic behavior [14), 20)], so the pressure equation of soil will obey Hooke's law, as follows,

$$P = -K\frac{\Delta V}{V} = K\left(\frac{\rho}{\rho_o} - 1\right) \tag{19}$$

where K is bulk modulus; $\Delta V/V$ is the volumetric strain; and ρ_o is the initial density of soil. Using the real value of K a stiff behavior of soil will be obtained. Therefore, K should be chosen as small as possible in order to ensure a near incompressibility condition and to avoid the stiff behavior (minimizing pressure fluctuations). In this study, we chose $K = 50\,\rho_o\, g\, Hmax$ in equation (19) (50 times the maximum initial pressure).The pressure gradient term in the Navier–Stokes equations has a symmetric form and it conserves both linear and angular momentum, more details could be found in (Khayyer et al., 2008) [21)]. The rate of change of deviatoric shear stress dS/dt can be calculated using shear modulus, μ, using the Jaumann rate from the following constitutive equation,

$$\frac{dS^{\alpha\beta}}{dt} = 2\mu\left(\varepsilon^{\alpha\beta} - \frac{1}{3}\delta^{\alpha\beta}\varepsilon^{\gamma\gamma}\right) + S^{\alpha\gamma}\omega^{\beta\gamma} + S^{\gamma\beta}\omega^{\alpha\gamma} \tag{20}$$

where $\varepsilon^{\gamma\gamma} = \varepsilon^{xx} + \varepsilon^{yy} + \varepsilon^{zz}$, is the strain rate tensor and $\omega^{\gamma\beta}$ is the rotation rate tensor. It can be defined by,

$$\varepsilon^{\alpha\beta} = \frac{1}{2}\left(\frac{\partial v^{\alpha}}{\partial x^{\beta}} + \frac{\partial v^{\beta}}{\partial x^{\alpha}}\right) \tag{21}$$

$$\omega^{\alpha\beta} = \frac{1}{2}\left(\frac{\partial v^{\alpha}}{\partial x^{\beta}} - \frac{\partial v^{\beta}}{\partial x^{\alpha}}\right) \tag{22}$$

Using the concept of the SPH approximation the SPH approximation of the strain rate tensor and the rotation rate tensor for particle i can be expressed as following:

$$\varepsilon_i^{\alpha\beta} = \frac{1}{2}\sum_{j=1}^{N}\left(\frac{m_j}{\rho_j}\left(v_i^{\alpha} - v_j^{\alpha}\right)\frac{\partial W_{ij}}{\partial x_i^{\beta}} + \frac{m_j}{\rho_j}\left(v_i^{\beta} - v_j^{\beta}\right)\frac{\partial W_{ij}}{\partial x_i^{\alpha}}\right) \tag{23}$$

$$\omega_i^{\alpha\beta} = \frac{1}{2}\sum_{j=1}^{N}\left(\frac{m_j}{\rho_j}\left(v_i^{\alpha} - v_j^{\alpha}\right)\frac{\partial W_{ij}}{\partial x_i^{\beta}} - \frac{m_j}{\rho_j}\left(v_i^{\beta} - v_j^{\beta}\right)\frac{\partial W_{ij}}{\partial x_i^{\alpha}}\right) \tag{24}$$

By combining Equations (20), (23) and (24), the deviatoric shear stress components can be calculated. Then, they are compared with the maximum shear stress ($S_f = c + P\, tan\phi$) in the plastic flow regime of the soil, which determined by the Mohr–Coulomb failure criterion. Here c is soil cohesion and ϕ is the angle of internal friction of the soil.

5. SOIL–WATER INTERACTION MODELING

When groundwater is seeping through the pores of a soil, viscous friction will produce drag on soil particles in the direction of water flow, so-called seepage force. This seepage force acts on the soil particles in addition to the gravitational force, and will be introduced into the momentum equations for soil and water as an external force according to the following model equation based on the Darcy's law:

$$f_{seepage} = \gamma_w\, n\,\frac{(v_{water} - v_{soil})}{k} \tag{25}$$

where γ_w is the unit weight of water; n is the porosity; and k is the soil permeability.

As saturated soil consists of soil and water mixed together while standard SPH models only handle one phase problem, it is necessary to develop a saturated soil model using in SPH simulation. This saturated soil model will be described as follows:

We assumed that the saturated soil domain in SPH can be divided into two separate phases, which are water phase and soil phase. The motion of SPH particles on each phase is solved separately using its own SPH governing equations, which are SPH for soil and SPH for water. These two-phases are then superimposed and the interaction between two-phases will be taken into account through the seepage force, which is introduced into the momentum equation as mentioned before. In addition, the water pressure is also allowed to contribute to the soil pressure during the overlapping procedure. This allows us to simulate the pore water pressure, which always exists in natural saturated soil. Accordingly, the momentum equations for saturated soil can be summarized as follows,

Momentum equation for soil phase:

$$\frac{Dv_i^\alpha}{Dt} = \sum_{j=1}^{N} m_j \left(\frac{s_i^{\alpha\beta}}{\rho_i^2} + \frac{s_j^{\alpha\beta}}{\rho_j^2} \right) \frac{\partial W_{ij}}{\partial x_i^\alpha} - \sum_{j=1}^{N} m_j \left(\frac{P_i}{\rho_i^2} + \frac{P_j}{\rho_j^2} \right) \frac{\partial W_{ij}}{\partial x_i^\alpha} - \sum_{a=1}^{N} m_a \frac{P_a}{\rho_i \rho_a} \frac{\partial W_{ia}}{\partial x_i^\alpha} + \sum_{a=1}^{N} m_a \frac{f_{ia}^{seepage}}{\rho_i \rho_a} W_{ia} + f_i^\alpha \quad (26)$$

Momentum equation for water phase:

$$\frac{Dv_i^\alpha}{Dt} = \sum_{b=1}^{N} m_b \left(\frac{\tau_a^{\alpha\beta}}{\rho_a^2} + \frac{\tau_b^{\alpha\beta}}{\rho_b^2} \right) \frac{\partial W_{ab}}{\partial x_a^\alpha} - \sum_{b=1}^{N} m_b \left(\frac{P_a}{\rho_a^2} + \frac{P_b}{\rho_b^2} \right) \frac{\partial W_{ab}}{\partial x_a^\alpha} - \sum_{i=1}^{N} m_i \frac{f_{ia}^{seepage}}{\rho_i \rho_a} W_{ia} + f_a^\alpha \quad (27)$$

where the subscripts i and j represent for soil particles while a and b are used for water particles. It is clear that these momentum equations of saturated soil are different from that of single phase. The presence of the seepage force in equations (26), (27), and the contribution of pressure from water to soil in equation (26) make them possible to simulate the effect of seepage force and pore water pressure in the saturated soil model, as a result the interaction between soil and water could be simulated through SPH. In order to damp out the unphysical stress fluctuation and to prevent shock waves and the penetration of particles through the boundaries, an artificial viscosity has been employed to the pressure term in the momentum equation. The most widely used type is proposed by Monaghan and Lattanzio (1985), and specified as follows,

$$\pi_{ij} = \begin{cases} \dfrac{-\alpha_1 \bar{c}_{ij} \phi_{ij} + \beta_1 \phi_{ij}^2}{\bar{\rho}_{ij}} & v_{ij}.x_{ij} < 0 \\ 0 & v_{ij}.x_{ij} \geq 0 \end{cases} \quad (28)$$

in which α_1 and β_1 are constants and were taken 1.0 and 1.0, respectively, and c represent the speed of sound. As well as having beneficial effects, artificial viscosity can also introduce unwanted numerical defects in some cases, among which the excess dissipation and false shearing torque in rotating flows (Dalrymple, and Knio, 2001) [22].

The momentum equations for saturated soil after introducing the artificial viscosity to the pressure term are:

Momentum equation for soil phase:

$$\frac{Dv_i^\alpha}{Dt} = \sum_{j=1}^{N} m_j \left(\frac{s_i^{\alpha\beta}}{\rho_i^2} + \frac{s_j^{\alpha\beta}}{\rho_j^2} \right) \frac{\partial W_{ij}}{\partial x_i^\alpha} - \sum_{j=1}^{N} m_j \left(\frac{P_i}{\rho_i^2} + \frac{P_j}{\rho_j^2} + \pi_{ij} \right) \frac{\partial W_{ij}}{\partial x_i^\alpha} + f_i^\alpha - \sum_{a=1}^{N} m_a \frac{P_a}{\rho_i \rho_a} \frac{\partial W_{ia}}{\partial x_i^\alpha} + \sum_{a=1}^{N} m_a \frac{f_{ia}^{seepage}}{\rho_i \rho_a} W_{ia} \quad (29)$$

Momentum equation for water phase:

$$\frac{Dv_i^\alpha}{Dt} = \sum_{b=1}^{N} m_b \left(\frac{\tau_a^{\alpha\beta}}{\rho_a^2} + \frac{\tau_b^{\alpha\beta}}{\rho_b^2} \right) \frac{\partial W_{ab}}{\partial x_a^\alpha} - \sum_{b=1}^{N} m_b \left(\frac{P_a}{\rho_a^2} + \frac{P_b}{\rho_b^2} + \pi_{ij} \right) \frac{\partial W_{ab}}{\partial x_a^\alpha} + f_a^\alpha - \sum_{i=1}^{N} m_i \frac{f_{ia}^{seepage}}{\rho_i \rho_a} W_{ia} \quad (30)$$

6. BOUNDARY CONDITIONS

In this paper a dynamic boundary condition is used to represent the boundary particles, which are forced to follow the governing equations (continuity, momentum and state equations), but they are fixed.

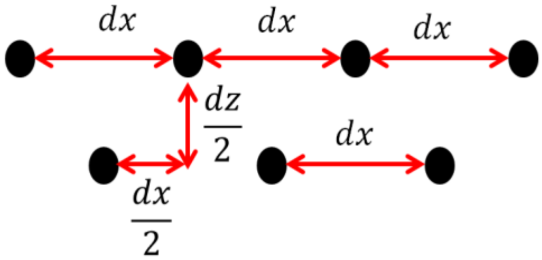

Fig.2 Arrangement of boundary particles

When the fluid particles are near to the boundary; the density of the boundary particles increases according to the continuity equation which leads to an increase in the pressure following the equation of state. Therefore the force exerted on the incoming fluid particles increases due to the pressure term in the momentum equation by generations of repulsion between the fluid and boundary particles [22]. The boundary particles are placed in a staggered manner in order to prevent the particle leakage as shown in **Fig.2**.

7. TIME INTEGRATION

Equations (13), (20), (29) and (30) are integrated using the Predictor- Corrector algorithm; this scheme predicts the evolution in time as,

$$\left.\begin{aligned} S_i^{n+1/2} &= S_i^n + (\Delta t/2) * DS_i(t) \\ \rho_i^{n+1/2} &= \rho_i^n + (\Delta t/2) * D\rho_i(t) \\ v_i^{n+1/2} &= v_i^n + (\Delta t/2) * Dv_i(t) \\ x_i^{n+1/2} &= x_i^n + (\Delta t/2) * v_i^n \end{aligned}\right\} \quad (31)$$

And the pressure is estimated according to the equation of state as,

$$P_i^{n+1/2} = f(\rho_i^{n+1/2}) \quad (32)$$

Values of υ, ρ, and x at the midpoint are then estimated using

$$\left.\begin{aligned} S_i^{n+\frac{1}{2}} &= S_i^n + (\Delta t/2) * DS_i(t)^{n+\frac{1}{2}} \\ \rho_i^{n+1/2} &= \rho_i^n + (\Delta t/2) * D\rho_i(t)^{n+1/2} \\ v_i^{n+\frac{1}{2}} &= v_i^n + (\Delta t/2) * Dv_i(t)^{n+\frac{1}{2}} \\ x_i^{n+1/2} &= x_i^n + (\Delta t/2) * v_i^{n+1} \end{aligned}\right\} \quad (33)$$

Finally, these values are calculated at the end of the time step using

$$\left.\begin{aligned} S_i^{n+1} &= 2 * S_i^{n+1/2} - S_i^n \\ \rho_i^{n+1} &= 2 * \rho_i^{n+1/2} - \rho_i^n \\ v_i^{n+1} &= 2 * v_i^{n+1/2} - v_i^n \\ x_i^{n+1} &= 2 * x_i^{n+1/2} - x_i^n \end{aligned}\right\} \quad (34)$$

And the pressure is calculated from density using:

$$P_i^{n+1} = f(\rho_i^{n+1}) \quad (35)$$

where Δt is the time step; and n is the time index. The stability of the Predictor-Corrector scheme is warranted using three criteria for time step. Following Monaghan [23], the time step Δt for a simulation is chosen to be the minimum from (CFL) condition, the condition of forcing terms and the condition of viscous diffusion term.

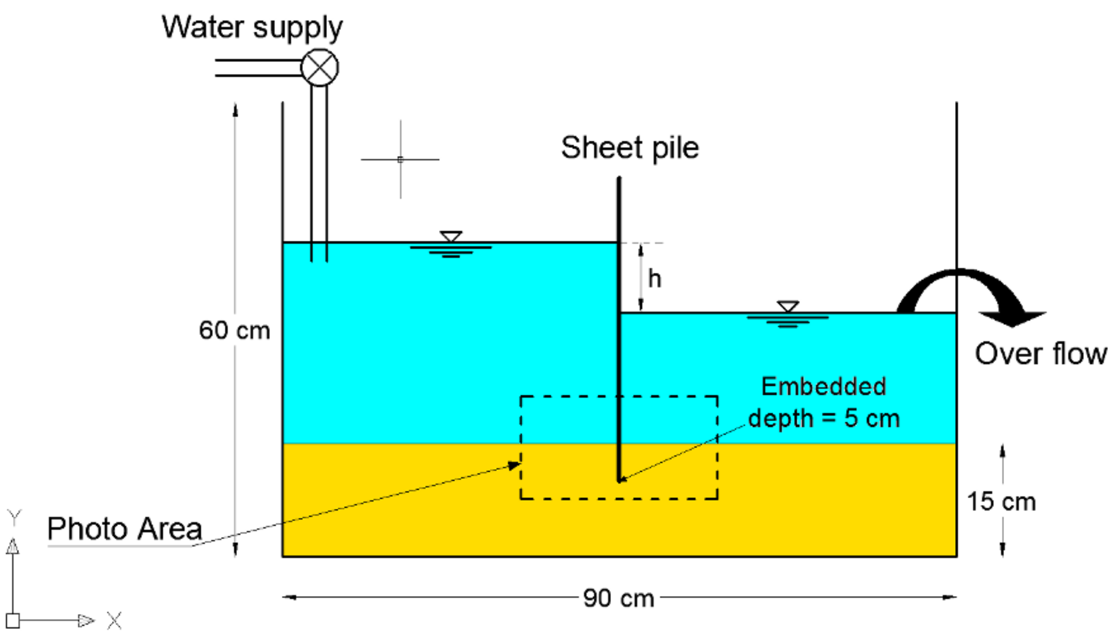

Fig.3 Schematic sketch of the experiment, Kodako et al. 2001

8. SEEPAGE FAILURE OF SANDY GROUND EXPERIMENT

(1) The model description

In order to evaluate our SPH model for soil–water interaction, simulations of the classical seepage failure problem in which a horizontal sandy ground with an embedded sheet pile have been carried out in this study. The experiment was done by Kodaka et al., 2001 [24]. Figure 2 shows a schematic sketch of the experimental setup.

A rectangular reservoir of 90 cm wide and 60 cm in depth contains 15 cm of a column of medium dense sand. The sheet pile is located in the middle of the tank with 1 cm thickness and its embedded in the soil equal 5 cm. The water head of upstream left side of sheet pile is gradually raised until the occurrence of seepage failure. The rate of raising the water head is 2 cm/min.

(2) Numerical simulations

The simulation of the seepage failure flows was carried out using the proposed SPH model.

The density ratio between soil density ρ_s, and water density ρ_w is taken as $\rho s/\rho_w = 1.54$. The soil is modeled by one type of particles with uniform material properties. These particles have the following properties: Young's modulus $E = 150$ MPa and Poisson's ratio $\upsilon = 0.3$, the porosity $n = 0.35$, the soil permeability $k = 0.05$ cm/s, soil cohesion $c = 0.5$ Mpa, and the angle of internal friction $\phi = 30^{o}$. The water particles have density of $\rho = 1.0$ g/cm^3, water unit weight $\gamma_w = 9.81$ kN/m^3, and viscosity $\mu = 10^{-3}$ Ns/m^2.

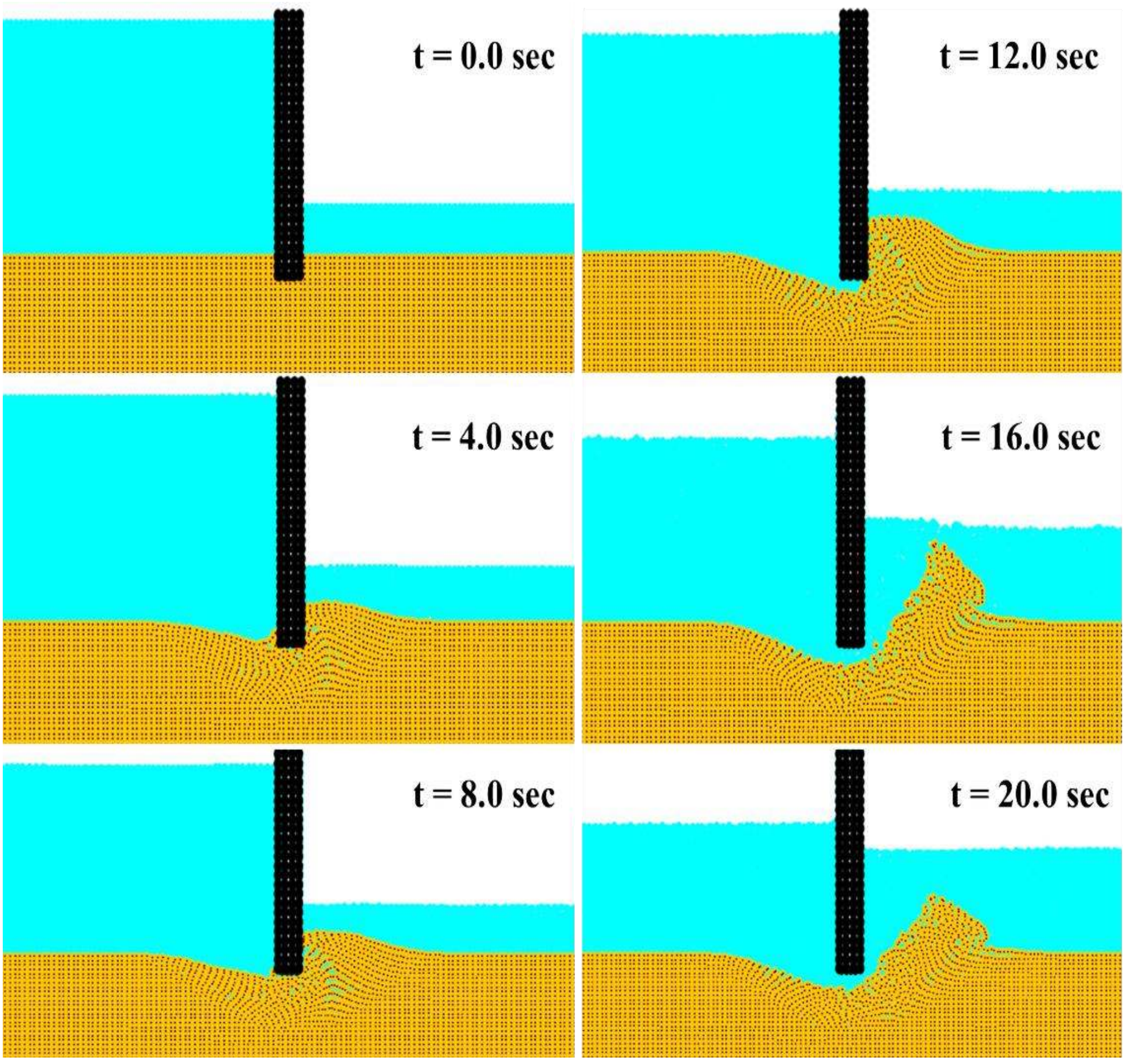

Fig.4 Series of snapshots of the erosion and seepage failure process (t = 0.0, 4.0, 8.0, 12.0, 16.0, 20.0 sec)

In total 5611 and 10064 particles representing the soil and water particles, respectively, with an initial smoothing length of 0.005 m was used.

(3) Results and analysis

The results of the simulation of the erosion and seepage failure process of saturated soil at selected times are shown in Fig.4.

In our model the saturated soil consisted of two-phases, water and soil, and each phase have to handle separately using its own SPH model in order to obtain the field variables of each particle. After the field variables of particles in each phase are computed, the interaction between soil and water can perform. The water pressure is permitted to contribute to the pressure of soil particles through the SPH summation, and thus the pore water pressure can be simulated. The seepage force is also computed as a function of the relative velocity between soil and water particles, and because of the presence of the seepage force in the momentum equations (29), (30), these water particles will force soil particles to move together, so the saturated soil mixture is effectively incompressible.

At the beginning of the simulation and due to the difference in water head between upstream and downstream sides, the bulk of soil on the downstream side loses its equilibrium of forces and rises to a certain degree, as a whole. Consequently, soil particles in the vicinity of the sheet pile wall move from the upstream to downstream side around the bottom tip of the sheet pile wall.

It is thought that, in the vicinity of the sheet pile wall, the downstream soil is subjected to an upward seepage force and is in a looser state than the original in situ condition. On the other hand, the upstream soil is subjected to a downward seepage force and could be in a somewhat denser state than at the beginning of the experiment. Such deformation is an unrecoverable damage for the soil and should be avoided. That is to say, the hydraulic head difference at deformation is important in the design of excavation with high ground water level from a practical point of view.

The results show that the model can successfully simulate the characteristics of seepage failure not only during deformation but also after the failure. As it is shown in the Fig. 4, the fluid particles are able to enter the sediment layer up to a certain depth, which is similar to seepage. The fluid particles fill up the voids between the sediment particles. The exerted forces by the fluid particles in the pores may be interpreted as a mix of buoyancy and lift forces. Also, we can see both the concentration of flow around the bottom of the sheet-pile and the evidence of high-speed flow on the downstream side due to curling induced by the erosion.

The result obtained by the SPH method is compared with the experimental image near the seepage failure conditions as shown in Fig.5.

From this comparison the results show that the current SPH model is sufficient to capture qualitatively the extremely large deformation and failure of soil, also the model is also in good quantitative agreement with the experiment, both in the position of the captured features and the time scale for their formation.

However, we have indicated differences in terms of the scouring shape around the sheet pile. Kodako et al. 2001 in their experiment indicates a steep scour shape in front of the sheet pile, but in the SPH simulation, a slight decrease in the angle of repose, after the soil collapse is observed as shown in Fig. 5.

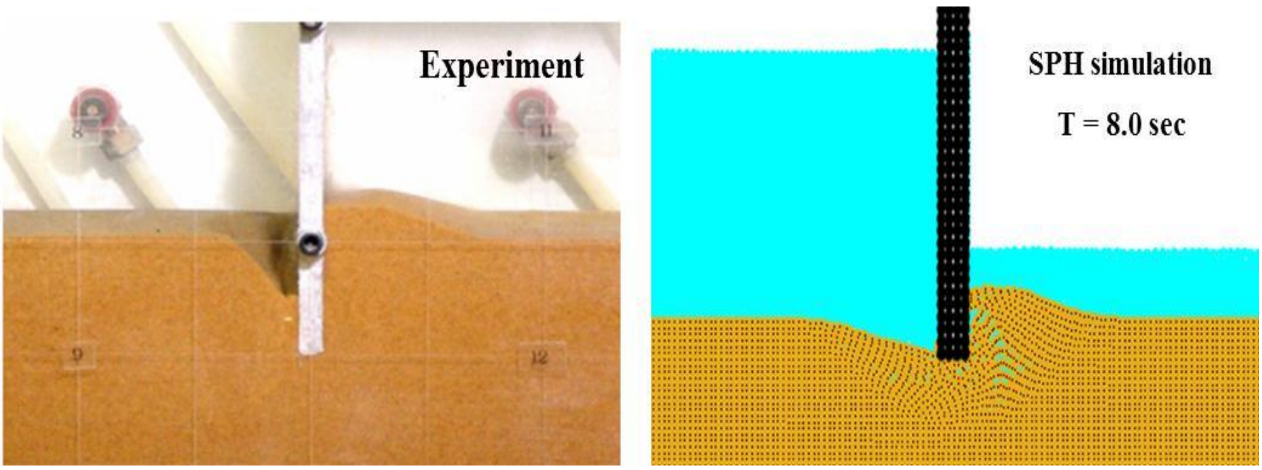

Fig.5 Comparison between the numerical results and the observed model test near the seepage failure conditions

It is probably because the number of particles is not adequate to give smooth and reliable results. Moreover, for simplicity, a zero dilation angle of sand is assumed, which led to a weaker soil in the SPH model (Chen et.al,) [25].

8. CONCLUSION

The development of an improved smoothed particle hydrodynamics to simulate the behavior of soil–water interaction has been described through this study. Water was modeled as a viscous fluid with weak compressibility the elastic–perfectly plastic model has been implemented in the SPH framework to model the soil materials. The interaction between soil and water was modeled by means of pore water pressure and seepage force.

The experiment of the seepage failure around a sheet-pile has been numerically simulated using the present model. The computational results were compared with the experimental results to check the capabilities of the proposed model.

The numerical results show that the SPH model can capture and describe the formation of soil erosion and scouring, but recognize the need for improvement to the constitutive modeling of soil, including saturated soil. Advantages of the method are its robustness, conceptual simplicity, and relative ease of incorporating new physics.

The results have shown that the extremely large deformation and failure of soil can be handled in SPH without any difficulties. The effect of pore water pressure and seepage force could be displayed well through SPH simulation. Although numerical results have not been quantitatively compared with experimental data due to the limitation of the experimental data, the calculations are stable and the results appear acceptable throughout.

This study suggests that SPH could be a powerful method for solving problems dealing large deformation and hydraulic collapse of the ground induced by water flow through the ground which could be significant in the destabilization of dam foundations during floods, liquefaction, and other catastrophic events.

ACKNOWLEDGMENT: This work was supported by JSPS KAKENHI Grant Number 15F15369.

REFERENCES

1) Lucy, L.: A numerical approach to testing the fission hypothesis, *Astronomical J.*, Vol. 82, pp. 1013–1024, 1977.
2) Gingold, R.A. and Monaghan, J. J.: Smoothed particle hydrodynamics: theory and application to nonspherical stars, *Mon. Not. Roy.* Astron .Soc, Vol. 181, pp. 375–389, 1977.
3) Libersky, L.D., and Petschek, A.G.: Smoothed particle hydrodynamics with strength of materials. *In Proceedings of the Next Free Lagrange Conference*, 395, Springer: New York, pp. 248–257, 1991.
4) Monaghan, J.J.: Simulating free surface flows with SPH. *J. Comput. Phys*, Vol.110, pp. 399–406, 1994.
5) Abdelrazek, A.M., Kimura, I., and Shimizu, Y.: Comparison between SPH and MPS Methods for Numerical Simulations of Free Surface Flow Problems, *Journal of Japan Society of Civil Engineers, Ser. B1 (Hydraulic Engineering)*, Vol.70 (4), pp. I_67-I_72, 2014.
6) Cummins, S.J. and Rudman, M.: A SPH projection method. *J. Comput. Phys,* Vol. 152, pp.584–607, 1999.
7) Gotoh, H., Khayyer, A., Ikari, H., Arikawa, T. and Shimosako, K.: On enhancement of Incompressible SPH method for simulation of violent sloshing flows, *Applied Ocean Res.*, Vol. 46, pp. 104–115, 2014.
8) Monaghan, J.J. and Kocharyan, A.: SPH simulation of multiphase flow. *Comput. Phys. Commune*, Vol. 87, pp. 225-235, 1995.
9) Monaghan, J.J.: SPH compressible turbulence. *Mon.Not. Roy.Astron.Soc*, Vol. 335 (3), pp.843-852, 2002.
10) Abdelrazek, A.M., Kimura, I., and Shimizu, Y.: Numerical Simulation of Snow Avalanches as a Bingham Fluid Flow Using SPH method, Proceedings of river flow 2014, *7th international conference on fluvial hydraulics, Lausanne, Switzerland*, pp. 1581–1587, CRC Press, Taylor & Francis Group, 2014.
11) Abdelrazek, A.M., Kimura, I., and Shimizu, Y. : Numerical simulation of a small-scale snow avalanche tests using non-Newtonian SPH model, *Journal of Japan Society of Civil Engineers, Ser. A2 (Applied Mechanics (AM))* Vol. 70, No.2, pp. I_681-I_690, 2014.
12) Abdelrazek, A.M., Kimura, I., and Shimizu, Y. : Numerical Simulation of Granular Flow Past Simple Obstacles using the SPH Method, *Journal of Japan Society of Civil Engineers, Ser. B1 (Hydraulic Engineering)*, Vol.71, No.4, pp. I_199-I_204, 2015.
13) Abdelrazek A.M., Kimura I., and Shimizu Y. : Simulation of three-dimensional rapid free-surface granular flow past different types of obstructions using the SPH method, *Journal of Glaciology*, Vol. 62, pp 335-347, 2016.
14) Bui Ha H., Sako K., and Fukagawa R.: Numerical simulation of soil–water interaction using smoothed particle hydrodynamics (SPH) method, Journal of Terramechanics, Vol.44, pp.339–346, 2007.
15) Bui, H. H., Fukagawa, R., Sako, K., and Wells, J. C.: Slope stability analysis and discontinuous slope failure simulation by elasto-plastic smoothed particle hydrodynamics (SPH), *Géotechnique*, Vol. 61 (7), pp. 565 –574, 2010.
16) Maeda, K., and Sakai, M.: Development of seepage failure analysis procedure of granular ground with Smoothed Particle Hydrodynamics (SPH) method, *Journal of applied mechanics*, Vol. 7, pp. 775-786, 2004.
17) Maeda, K., Sakai, M., and Imase, T.: Erosion and seepage failure analysis of ground with evolution of bubbles using SPH, *Prediction and Simulation Methods for Geohazard Mitigation*, 185-191, 2009.
18) Liu G.R., and Liu M. B.: Smoothed particle hydrodynamics: a mesh-free particle method, *World Scientific*; 2003.
19) Wendland, H.: Piecewiese polynomial, positive definite and compactly supported radial functions of minimal degree, *Advances in computational* Mathematics, Vol.4 (1), pp. 389- 396, 1995.
20) Yaidel R.L., Dirk R., and Carlos R. M.: Dynamic refinement for SPH simulations of post-failure flow of non-cohesive soil, *7th international SPHERIC workshop*,

Prato, Italy, May 29-31, 2012.
21) Khayyer, A., Gotoh, H. and Shao, S.: Corrected Incompressible SPH method for accurate water-surface tracking in breaking waves, Coastal Eng., Vol. 55, pp. 236-250, 2008.
22) Dalrymple, R.A., and Knio, O.: SPH modelling of water waves. *Proc. Coastal Dynamic*s, 779-787, Sweden, 2001.
23) Monaghan, J. J.: On the problem of penetration in particle methods. *J. Comput. Phys*, Vol.82 pp.1-15, 1989.
24) Kodaka, T., Oka, F. and Morimoto, R.: Seepage failure analysis of sandy ground using a liquefaction analysis method based on finite deformation theory, *Computational Mechanics, S.Valliappan and N.Khailili eds., Elsevier Proc. The first Asian-Pacific Congress on Computational mechanics*, Sydney, Australia, 20-23 Nov.2001. Vol.1. pp. 387-392, 2001.
25) Chen, W., and Qiu, T.: Numerical Simulations for Large Deformation of Granular Materials Using Smoothed Particle Hydrodynamics Method, *Int. J. Geomech.,*Vol.12(2), 127–135, 2012.

(Received June 24, 2016)